Electronic Journal of Mathematical Analysis and Applications
Vol. 6(2) July 2018, pp. 86-100.
ISSN: 2090-729X(online)
http://fcag-egypt.com/Journals/EJMAA/

VIBRATION CONTROL OF A NONLINEAR DYNAMICAL SYSTEM EXCITED AT SIMULTANEOUS RESONANCE CASE

W. A. EL-GANAINI

Abstract. Within this article, an active Positive Position Feedback (PPF) controller is applied to suppress the horizontal vibration of a nonlinear magnetic levitation system. The purposed controller is designed to have a natural frequency equal to the excitation frequency of the magnetic levitation system. The multiple scales perturbation method is adopted to derive two nonlinear algebraic equations that describe the whole system vibration amplitudes in terms of the system and controller parameters. The solution's stability is studied utilizing the indirect method of Lyapunov. Then, numerical validations for the obtained analytical results are performed. The analyses illustrated a good agreement between the numerical and analytical solution, and showed the high efficiency of the PPF controller in suppressing the system vibrations in the presence of primary resonance and 1:1 internal resonance. Eventually, a comparison with previously published work is included.

1. Introduction

One of the high advanced technologies is the magnetic levitation systems which have various engineering applications like clean energy in wind turbines, transportation systems in magnetic levitation train, building facilities in fans, nuclear engineering in the centrifuge of nuclear reactor, civil engineering in elevators?etc. In all these applications, we can find common features such as the lack of contact and thus no friction. The oscillatory motions of such applications should be eliminated or suppressed to increases the efficiency and the life of the system and reduces the maintenance costs. For all these reasons, the technique of passive and active control is applied to suppress the nonlinear vibration of those systems to its minimum possible level.
Jo et al. [1-2], studied dynamic vibration absorber depending on quadratic nonlinear coupling as passive controller to reduce the vibration amplitude of primary and parametric resonance of a nonlinear oscillator. The applied absorber is a pendulum with tip mass that attached vertically to the body and was designed to have

2010 *Mathematics Subject Classification.* 34C15, 34C23, 34C25, 34C60, 34F15,37C75, 37N35, 70K30, 70K40, 70K42.
Key words and phrases. Magnetic levitation body, Active vibration control, stability, Positive position feedback, Simultaneous resonance.
Submitted Nov. 5, 2017.

a natural frequency in the neighborhood of twice that of the main system. Furthermore, the authors showed experimentally that the nonlinear vibration absorber reduced the primary resonance amplitude with a reduction ratio of about 45%, but in the case of principal parametric resonance, the steady state amplitude became close to zero. Yabuno et al. [3] studied the effect of parametric resonance due to asymmetric nonlinearity of restoring force. They concluded that the instability region of the trivial steady state due to the parametric excitations depends on the value of subharmonic excitation with order half. Warminski et al. [4] discussed an active positive position feedback (PPF) controller to mitigate the nonlinear vibrations of a nonlinear composite beam. The PPF controller exhibited high efficiency in suppressing the system vibration amplitude. Shin et al. [5] investigated the active vibration control of clamped beams using PPF controllers with a pair-actuator (sensor/moment). They showed that the PPF controller has alleviated the system instability produced by the sensor/moment pair actuator. Eissa and Sayed [6-7] presented a comparison between active and passive vibration control of non-linear simple pendulum. The authors showed that the velocity feedback is better than the quadratic and cubic velocity feedback for transversally tuned absorber, where the active controller effectiveness decreases with increasing the order of velocity feedback. In addition, they applying acceleration and displacement feedback for longitudinal tuned absorber and provided that each of them depends on the nature of the system to be controlled. Furthermore, Eissa and Sayed [8], studied the vibration reduction of a three DOF nonlinear spring pendulum using an active vibration control. Amer et al. [9-10] applied two simple active control methods based on the linear velocity and acceleration feedback to suppress the nonlinear vibration of a an aircraft twin-tail system when subjected to harmonic, parametric, and external excitation. They concluded that the acceleration feedback has high efficiency in reducing the twin-tail system vibrating. Sayed and Kamel [11] discussed the vibration control of a nonlinear dynamical system via an active control algorithm depending on the 1:2 and 1:3 internal resonance cases. El-Ganaini et al. [12-13], discussed chaotic vibration suppression via time delay absorber of a beam under multi-parametric excitations. They concluded the absorber effectiveness (E_a) is infinity theoretically at simultaneous resonance case ($\Omega = 2\omega_1$ and $\omega_1 = \omega_2$), while at simultaneous resonance case ($\Omega_1 = \omega_1$ and $\Omega_1 = \omega_2$) E_a is about 700. An active controller for suppressing a nonlinear system vibration by applying PPF is studied by El-Ganaini et al. [14]. They showed that the good benefit of using this controller is that if its natural frequency is tuned in the neighborhood of the measured excitation frequency, its effectiveness (E_a) can be reached about 625. As the PPF controller has high feasibility and wide applicability in nonlinear vibration control, it is still the up to date and a common controller in suppressing the vibrations of different nonlinear dynamical systems, where Eissa and Saeed [15], and Saeed and Kamel [16], recently published two papers concerning the lateral vibration control of the nonlinear Jeffcott rotor system. In this paper, PPF controller is connected to the nonlinear system presented in Refs [1-2] as shown in Fig. 1. In this system, the vertically levitated body is guided by horizontal magnetic forces on both sides, where one of these magnets is under an external periodic excitation. The frequency response equations that describe the steady state oscillations of the given system is derived applying MSPT method [17]. The stability analysis is performed to determine the stable and unstable regions for both system and controller. A comparison

between the obtained analytical results and the numerical simulations is held and showed a good agreement.

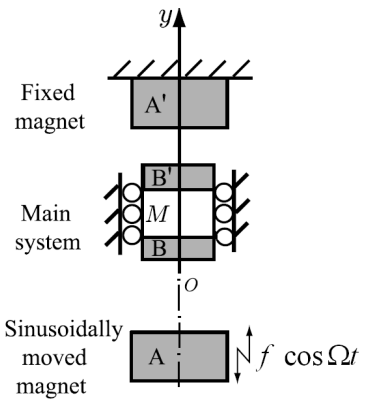

FIGURE 1. Magnetic Levitation system

2. Perturbation analysis

The nonlinear differential equation governing the magnetic levitation system vibrations under periodic primary excitation is given as follows (See Ref. [1]):

$$\ddot{y} + 2\mu_1\dot{y} + y + \alpha y^3 = 2k_2 fy\cos(\Omega t) + 3k_3 fy^2\cos(\Omega t) - 3k_3 f^2 y\cos^2(\Omega t) + k_1 f\cos(\Omega t) - k_2 f^2\cos^2(\Omega t) + k_3 f^3\cos^3(\Omega t) \quad (1)$$

After the PPF controller is applied to the suggested system [14, 15], the modified equations of motion will be in the form:

$$\ddot{y} + 2\mu_1\dot{y} + y + \alpha y^3 = 2k_2 fy\cos(\Omega t) + 3k_3 fy^2\cos(\Omega t) - 3k_3 f^2 y\cos^2(\Omega t) + k_1 f\cos(\Omega t) - k_2 f^2\cos^2(\Omega t) + k_3 f^3\cos^3(\Omega t) + c_1 z \quad (2.a)$$

$$\ddot{z} + 2\mu_2\dot{z} + {\omega_2}^2 z = c_2 y \quad (2.b)$$

In equations (2.a) and (2.b), a new scaling for the system and controller parameters depending on their values is considered such that:

$$\mu_1 = \varepsilon^2\hat{\mu}_1, \quad \mu_2 = \varepsilon^2\hat{\mu}_2, \quad c_1 = \varepsilon^2\hat{c}_1, \quad c_2 = \varepsilon^2\hat{c}_2, \quad f = \varepsilon^3\hat{f} \quad (3)$$

Applying the MSPT [17], we suppose the uniform expansion of y and z as:

$$y(T_0, T_1; \varepsilon) = \varepsilon y_1(T_0, T_1) + \varepsilon^3 y_2(T_0, T_1) + O(\varepsilon^5) \quad (4.a)$$

$$z(T_0, T_1; \varepsilon) = \varepsilon z_1(T_0, T_1) + \varepsilon^3 z_2(T_0, T_1) + O(\varepsilon^5) \quad (4.b)$$

where $T_0 = t, T_1 = \varepsilon^2 t$ are the fast and slow time scales respectively. In terms of T_0 and T_1, the time derivatives are transformed into the following:

$$\frac{d}{dt} = D_0 + \varepsilon^2 D_1, \quad \frac{d^2}{dt^2} = {D_0}^2 + 2\varepsilon^2 D_1 D_0; \quad D_i = \frac{\partial}{\partial T_i}, \quad i = 0, 1 \tag{5}$$

Substituting equations (3) to (5) into equations (2.a) and (2.b) and equating coefficients of the powers of ε, the following set of linear differential equations are obtained

$O(\varepsilon)$:

$$({D_0}^2 + 1)y_1 = 0 \tag{6.a}$$

$$({D_0}^2 + {\omega_2}^2)z_1 = 0 \tag{6.b}$$

$O(\varepsilon^3)$:

$$({D_0}^2 + 1)y_2 = -2D_1 D_0 y_1 - 2\hat{\mu_1} D_0 y_1 - \alpha {y_1}^3 + \frac{k_1 \hat{f}}{2}(e^{i\Omega T_0} + e^{-i\Omega T_0}) + \hat{c}_1 z_1 \tag{7.a}$$

$$({D_0}^2 + {\omega_2}^2)z_2 = -2D_1 D_0 z_1 - 2\hat{\mu_2} D_0 z_1 + \hat{c}_2 y_1 \tag{7.b}$$

The general solutions of equations (6.a) and (6.b) are expressed in the complex form as:

$$y_1(T_0, T_1) = A_1(T_1)e^{iT_0} + \bar{A}_1(T_1)e^{-iT_0} \tag{8.a}$$

$$z_1(T_0, T_1) = A_2(T_1)e^{i\omega_2 T_0} + \bar{A}_2(T_1)e^{-i\omega_2 T_0} \tag{8.b}$$

where the quantities $A_1(T_1)$ and $A_2(T_1)$ are unknown complex functions in T_1. Substituting equations (8) into equations (7), we get the following:

$$\begin{aligned}({D_0}^2 + 1)y_2 = (&-2iD_1 A_1 - 2i\hat{\mu_1} A_1 - 3\alpha {A_1}^2 \bar{A_1})e^{iT_0} - \alpha {A_1}^3 e^{3iT_0} + \frac{k_1 \hat{f}}{2} e^{i\Omega T_0} \\ &+ \hat{c_1} A_2 e^{i\omega_2 T_0} + cc\end{aligned} \tag{9.a}$$

$$({D_0}^2 + {\omega_2}^2)z_2 = (-2i\omega_2 D_1 A_2 - 2i\hat{\mu_2}\omega_2 A_2)e^{i\omega_2 T_0} + \hat{c_2} A_1 e^{iT_0} + cc \tag{9.b}$$

where cc denotes the complex conjugate of the preceding terms. The particular solutions of equations (9) are

$$y_2(T_0, T_1) = \frac{\alpha}{8}{A_1}^3 e^{3iT_0} + \frac{k_1}{2(1-\Omega^2)}\hat{f}e^{i\Omega T_0} + \frac{\hat{c_1}}{1-{\omega_2}^2}A_2 e^{i\omega_2 T_0} + cc \tag{10.a}$$

$$z_2(T_0,T_1)=\frac{\hat{c_2}}{{\omega_2}^2-1}A_1e^{iT_0}+cc \tag{10.b}$$

The normalized resonance cases that concluded from the approximate solution in equations (10) are reported as:

(i) Primary Resonance: $\Omega=1$
(ii) Internal Resonance: $\omega_2=1$
(iii) Simultaneous resonance: $\Omega=1$ and $\omega_2=1$

The case of simultaneous resonance case ($\Omega=1$ and $\omega_2=1$) is considered in this work because it represents the worst resonance case. The stability of the vibrating system near this simultaneous resonance is studied by proposing detuning parameters σ_1 and σ_2 such that:

$$\Omega=1+\sigma_1=1+\varepsilon^2\hat{\sigma_1} \tag{11.a}$$

$$\omega_2=1+\sigma_2=1+\varepsilon^2\hat{\sigma_2} \tag{11.b}$$

The solvability conditions of equations (9) can be obtained by inserting equations (11) into equations (9), and eliminating the secular and small-divisor terms, the following are obtained:

$$-2iD_1A_1-2i\hat{\mu}_1A_1-3\alpha A_1^2\overline{A_1}+\frac{k_1\hat{f}}{2}e^{i\hat{\sigma}_1T_1}+\hat{c}_1A_2e^{i\hat{\sigma}_2T_1}=0 \tag{12.a}$$

$$-2i\omega_2D_1A_2-2i\hat{\mu}_2\omega_2A_2+\hat{c}_2A_1e^{-i\hat{\sigma}_2T_1}=0 \tag{12.b}$$

To analyze equation (12), we can express $A_1(T_1)$ and $A_2(T_1)$ in the polar form as follows:

$$A_1(T_1)=\frac{\hat{a}_1}{2}e^{i\beta_1}\Rightarrow D_1A_1(T_1)=\frac{1}{2}\hat{a}'_1e^{i\beta_1}+\frac{i}{2}a_1{\beta'}_1e^{i\beta_1} \tag{13.a}$$

$$A_2(T_1)=\frac{\hat{a}_2}{2}e^{i\beta_2}\Rightarrow D_1A_2(T_1)=\frac{1}{2}\hat{a}'_2e^{i\beta_2}+\frac{i}{2}a_2{\beta'}_2e^{i\beta_2} \tag{13.b}$$

where $\hat{a_1}$ and $\hat{a_2}$ are the steady-state amplitudes of the main system and controller, respectively, and β_1 and β_2 are the phases of the main system and controller, respectively. Substituting equations (13) into equations (12), we get

$$-i\hat{a}'_1e^{i\beta_1}+\hat{a}_1{\beta'}_1e^{i\beta_1}-i\hat{\mu}_1\hat{a}_1e^{i\beta_1}-\frac{3}{8}\alpha\hat{a}_1^3e^{i\beta_1}+\frac{k_1\hat{f}}{2}e^{i\hat{\sigma}_1T_1}+\frac{\hat{c}_1}{2}\hat{a}_2e^{i(\hat{\sigma}_2T_1+\beta_2)}=0 \tag{14.a}$$

$$-i\omega_2\hat{a}'_2e^{i\beta_2}+\omega_2\hat{a}_2{\beta'}_2e^{i\beta_2}-i\hat{\mu}_2\omega_2\hat{a}_2e^{i\beta_2}+\frac{\hat{c}_2}{2}\hat{a}_1e^{-i(\hat{\sigma}_2T_1-\beta_1)}=0 \tag{14.b}$$

Return back every scaled parameter into its original form, we have

$$\hat{\mu}_1=\frac{\mu_1}{\varepsilon^2},\hat{\mu}_2=\frac{\mu_2}{\varepsilon^2},\hat{c}_1=\frac{c_1}{\varepsilon^2},\hat{c}_2=\frac{c_2}{\varepsilon^2},\hat{f}=\frac{f}{\varepsilon^3},\hat{a}_1=\frac{a_1}{\varepsilon},\hat{a}_2=\frac{a_2}{\varepsilon},\hat{\sigma}_1=\frac{\sigma_1}{\varepsilon^2},\hat{\sigma}_2=\frac{\sigma_2}{\varepsilon^2} \tag{15}$$

Substituting equation (15) into equations (14), we get that:

$$-i\dot{a}_1e^{i\beta_1}+a_1\dot{\beta}_1e^{i\beta_1}-i\mu_1a_1e^{i\beta_1}-\frac{3}{8}\alpha a_1^3e^{i\beta_1}+\frac{k_1f}{2}e^{i\sigma_1t}+\frac{c_1}{2}a_2e^{i(\sigma_2t+\beta_2)}=0 \tag{16.a}$$

$$-i\omega_2\dot{a}_2e^{i\beta_2}+\omega_2a_2\dot{\beta}_2e^{i\beta_2}-i\mu_2\omega_2a_2e^{i\beta_2}+\frac{c_2}{2}a_1e^{-i(\sigma_2t-\beta_1)}=0 \tag{16.b}$$

Dividing equations (16.a) and (16.b) by $e^{i\beta_1}$ and $e^{i\beta_2}$, respectively, and separating the real and imaginary parts leads to the following equations:

$$\dot{a}_1=-\mu_1a_1+\frac{c_1}{2}a_2\sin\varphi_2+\frac{k_1f}{2}\sin\varphi_1 \tag{17.a}$$

$$a_1\dot{\beta}_1=\frac{3\alpha}{8}a_1^3-\frac{c_1}{2}a_2\cos\varphi_2-\frac{k_1f}{2}\cos\varphi_1 \tag{17.b}$$

$$\dot{a}_2=-\mu_2a_2-\frac{c_2}{2\omega_2}a_1\sin\varphi_2 \tag{17.c}$$

$$a_2\dot{\beta}_2=-\frac{c_2}{2\omega_2}a_1\cos\varphi_2 \tag{17.d}$$

$$where\varphi_1=\sigma_1t-\beta_1\ ,\ \varphi_2=\sigma_2t-\beta_1+\beta_2 \tag{18}$$

Eliminating $\dot{\beta}_1$ and $\dot{\beta}_2$ from equations (17) using equations (18), we get the following autonomous system of equations:

$$\dot{a}_1=-\mu_1a_1+\frac{c_1}{2}a_2\sin\varphi_2+\frac{k_1f}{2}\sin\varphi_1 \tag{19.a}$$

$$\dot{\varphi}_1=\sigma_1-\frac{3\alpha}{8}a_1^2+\frac{c_1}{2}\frac{a_2}{a_1}\cos\varphi_2+\frac{k_1f}{2}\frac{1}{a_1}\cos\varphi_1 \tag{19.b}$$

$$\dot{a}_2=-\mu_2a_2-\frac{c_2}{2\omega_2}a_1\sin\varphi_2 \tag{19.c}$$

$$\dot{\varphi}_2 = \sigma_2 - \frac{3\alpha}{8}a_1^2 + \frac{c_1}{2}\frac{a_2}{a_1}\cos\varphi_2 + \frac{k_1 f}{2}\frac{1}{a_1}\cos\varphi_1 - \frac{c_2}{2\omega_2}\frac{a_1}{a_2}\cos\varphi_2 \tag{19.d}$$

The behavior of the system response before and after control can be described by the obtained the steady state equations from (19), which describe the modulation of amplitudes and phases of the vibrating system.

3. Equilibrium Solution and stability analysis

The steady state response of both system and controller can be obtained, by setting $\dot{a_1} = \dot{a_2} = \dot{\varphi_1} = \dot{\varphi_2} = 0$ into equation (19), yield:

$$\mu_1 a_1 = \frac{c_1}{2}a_2\sin\varphi_2 + \frac{k_1 f}{2}\sin\varphi_1 \tag{20.a}$$

$$-\sigma_1 a_1 + \frac{3\alpha}{8}a_1^3 = \frac{c_1}{2}a_2\cos\varphi_2 + \frac{k_1 f}{2}\cos\varphi_1 \tag{20.b}$$

$$-\mu_2 a_2 = \frac{c_2}{2\omega_2}a_1\sin\varphi_2 \tag{20.c}$$

$$(\sigma_2 - \sigma_1)a_2 = \frac{c_2}{2\omega_2}a_1\cos\varphi_2 \tag{20.d}$$

Eliminating φ_1 and φ_2 from equations (20), we get:

$$\frac{c_2^2}{4\omega_2^2}a_1^2 = (\mu_2^2 + (\sigma_2 - \sigma_1)^2)a_2^2 \tag{21}$$

$$\frac{k_1^2 f^2}{4}a_1^2 = (\mu_1 a_1^2 + \frac{c_1\mu_2\omega_2}{c_2}a_2^2)^2 + (-\sigma_1 a_1^2 + \frac{3\alpha}{8}a_1^4 - \frac{c_1\omega_2(\sigma_2 - \sigma_1)}{c_2}a_2^2)^2 \tag{22}$$

The steady state solution of the given system can be obtained by solving the frequency-response equations (21) and (22) in terms of the system and controller parameters. The stability of the equilibrium points is studied by checking the Eigenvalues of the Jacobian matrix. So, let:

$$a_n = a_{n1} + a_{n0} \quad \textit{and} \quad \varphi_n = \varphi_{n1} + \varphi_{n0}; \quad (n = 1, 2) \tag{23}$$

where a_{n0} and φ_{n0} are the steady state solutions for both the system and controller, a_{n1} and φ_{n1} are small perturbation about the steady state solutions (a_{n0} and φ_{n0}). Substituting equations (23) into equations (19), keeping only the linear terms in a_{n1} and φ_{n1}, we get the following linearized system:

$$\begin{bmatrix} \dot{a}_{11} \\ \dot{\varphi}_{11} \\ \dot{a}_{21} \\ \dot{\varphi}_{21} \end{bmatrix} = \begin{pmatrix} r_{11} & r_{12} & r_{13} & r_{14} \\ r_{21} & r_{22} & r_{23} & r_{24} \\ r_{31} & r_{32} & r_{33} & r_{34} \\ r_{41} & r_{42} & r_{43} & r_{44} \end{pmatrix} \begin{bmatrix} a_{11} \\ \varphi_{11} \\ a_{21} \\ \varphi_{21} \end{bmatrix} \tag{24}$$

where the above square matrix is the system Jacobian matrix and its coefficients $r_{ij} : \{i, j = 1, 2, 3, 4\}$ are given in the appendix. The stability of the steady-state solutions of equations (21) and (22) depends on the Eigenvalues of the Jacobian matrix. Accordingly, we can be obtained the following characteristic equation:

$$\lambda^4 + \zeta_1\lambda^3 + \zeta_2\lambda^2 + \zeta_3\lambda + \zeta_4 = 0 \tag{25}$$

where λ denotes the Eigenvalues of the Jacobian matrix and $\zeta_1,\ \zeta_2,\ \zeta_3,\ \zeta_4$ are given in the appendix. According to the Routh-Hurwitz criterion, the equilibrium solutions (a_{n0} and φ_{n0}) is asymptotically stable if and only if:

$$\zeta_1 > 0 \ \ , \ \ \zeta_1\zeta_2 - \zeta_3 > 0 \ \ , \ \ \zeta_3(\zeta_1\zeta_2 - \zeta_3) - \zeta_1^2\zeta_4 > 0 \ \ , \ \ \zeta_4 > 0 \tag{26}$$

4. Numerical Simulations

For the given system parameters, the selected values are given by: $\mu_1 = 0.02, \mu_2 = 0.001, \omega_2 = 1, \alpha = 0.894, k_1 = 0.5, k_2 = 0.547, k_3 = 0.447, c_1 = c_2 = 0.3$ and $f = 0.05$, unless specifying otherwise. Fig. 2 shows the main system (i.e. magnetic levitation system) time history without control when $\Omega = 1$, where the steady state vibration amplitude is about 0.3394, while the controlled main system and controller amplitudes time history at $\Omega = 1$ is shown in Fig. 3. For different initial conditions, we found that the system steady state amplitude is insensitive to initial conditions. Also from Fig. 3, we see that the system steady state amplitude is about 0.0015, and the controller effectiveness E_a is about 226. The comparison between analytical and numerical solution for both the main system and the controller is shown in Figs 4 and 5. A good validation of the frequency response curves is plotted to compare analytical solution using MSPT method and the numerical simulation applying Runge-Kutta algorithm. Fig. 6 shows a comparison for the force response curves of the main system and the controller and we conclude that both solutions are in a good agreement.

5. Effect of different parameters on the system response

In this section, the behavior of the vibrating system is studied through the effects of different parameters on the main system and controller. The frequency response curves for the main system before control application gives open loop case as shown in Fig. 7, and we find the steady state amplitude is a monotonic increasing function to the excitation force amplitude. In addition, when the force amplitude increases, the curve is bent to the right denoting hardening effect and the jump phenomenon appears clearly due to the domination of the nonlinearity.

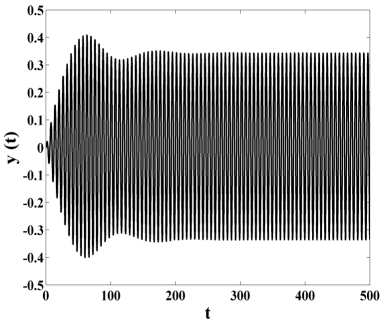

FIGURE 2. Main system time history without control ($\Omega = 1$)

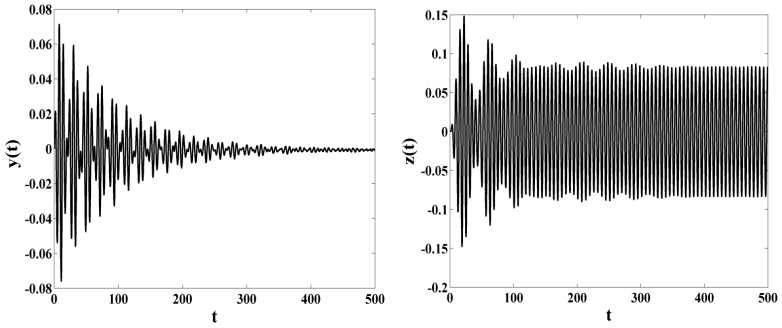

FIGURE 3. Main system and controller time histories with control ($\Omega = 1$)

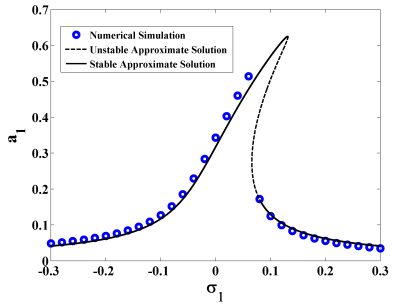

FIGURE 4. Frequency response curve for the system without control at f = 0.05

Fig. 8 illustrates the frequency response curves for the main system with control, which gives closed loop case. It is found two peaks are produced at the values $\sigma_1 = -0.11$ and $\sigma_1 = 0.23$, so they are creating a bandwidth in-between about 0.44 . In addition, in this figure, the minimum system amplitude occurs at $\sigma_1 = 0$ and the most effective operating point for the controller is to work within $\sigma_1 = \pm 0.1$ approximately.

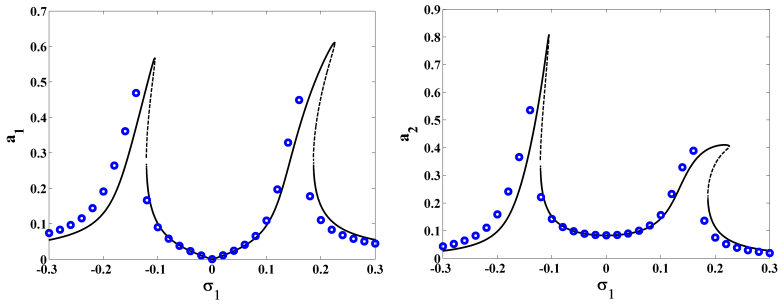

FIGURE 5. Main system and controller frequency response curves at f = 0.05

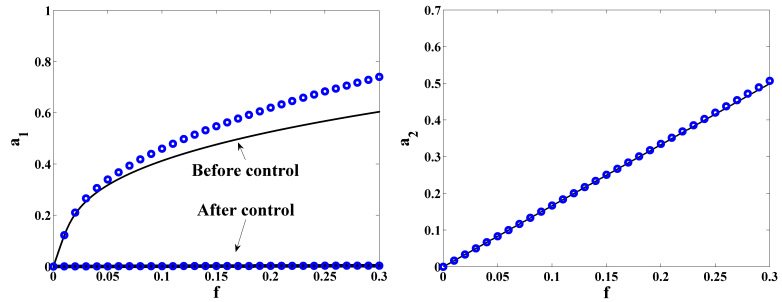

FIGURE 6. Main system and controller frequency response curves at $\sigma_1 = \sigma_2 = 0$

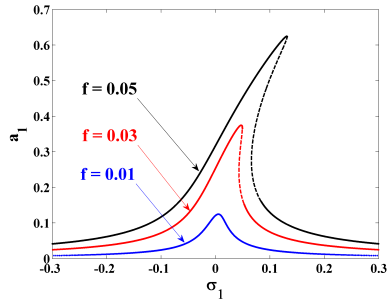

FIGURE 7. Frequency response curves of the system without control for different values of **f**

Figs 9 and 10 show the effects of different values of the control signal gain c_1 and the feedback signal gain c_2 on the frequency response curves for both the main system and the controller. It is clear from increasing c_1 and c_2 that the bandwidth between the two peaks increases which gives more flexibility for the controller job. This can increase the safety factor because the value of σ_1 may deviate from 0 and go towards one of the values where the peaks are located. It is to be noticed that

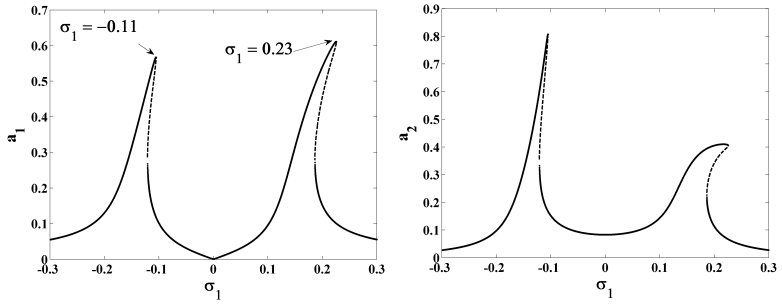

FIGURE 8. Frequency response curves of the main system with control for $\sigma_2 = 0$

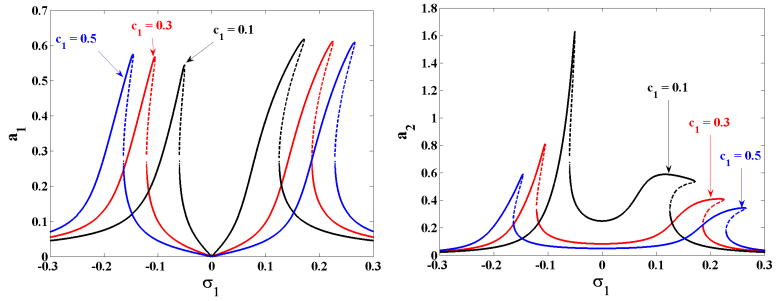

FIGURE 9. Frequency response curves of the main system and controller at different values of c_1

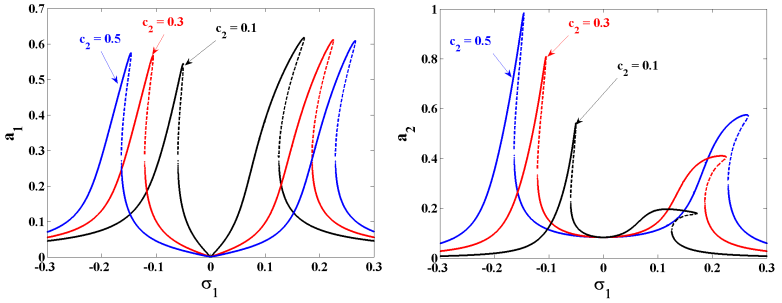

FIGURE 10. Frequency response curves of the main system and controller at different values of c_2

the peaks values are not affected for the main system by variation of either c_1 or c_2.

The effects of different values of the controller linear damping μ_2 on the frequency response curves are demonstrated in Fig. 11. From this figure, we can see that increasing the parameter μ_2 reduces the amplitudes of the two peaks of the main system and the controller. Also, we have the main system amplitude at $\sigma_1 = 0$

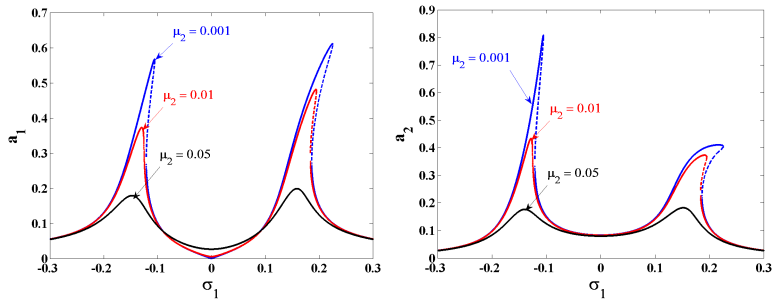

FIGURE 11. Frequency response curves of the main system and controller at different values of μ_2

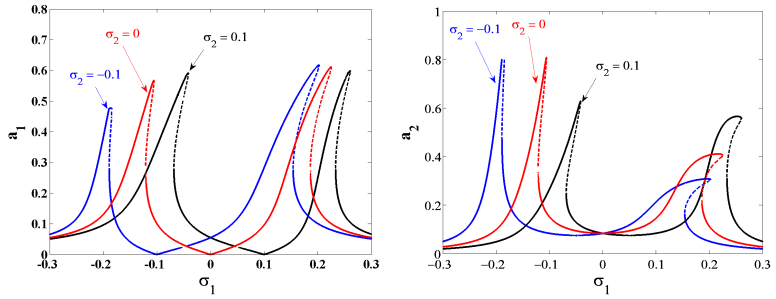

FIGURE 12. Frequency response curves of the main system and controller at different values of σ_2

increases slightly when the energy transfer between the main system and controller decreases. It is also noted that the bandwidth is not affected by changing μ_2.

Fig. 12 shows the effects of varying the detuning parameter σ_2 on the frequency response curves of both the system and the controller. We note that the system amplitude is at its minimum value when $-0.1 \leq \sigma_2 = \sigma_1 \leq 0.1$. We conclude that if we could tune the natural frequency of controller ω_2 to the value of the measured excitation frequency Ω, we can always get the relation $\sigma_2 = \sigma_1$ to achieve a minimum value of the system amplitude.

The force response curves for the main system without and with the control is shown Fig. 13. From this figure we observe that the relation between the system amplitude and the excitation force without control is a nonlinear relation which produces large system amplitudes for a slight increase in the excitation force. When the control is applied, the relation became horizontal, so increasing the excitation force largely produces an extremely small change in the system amplitude denoting a saturation case. On the other hand, the controller amplitude increases linearly with the excitation force.

6. CONCLUSIONS

In this paper, MSPT technique was applied to derive an approximate solution for the magnetic levitation system which is coupled to an active positive position feedback (PPF) controller. A system of four first order differential equations was

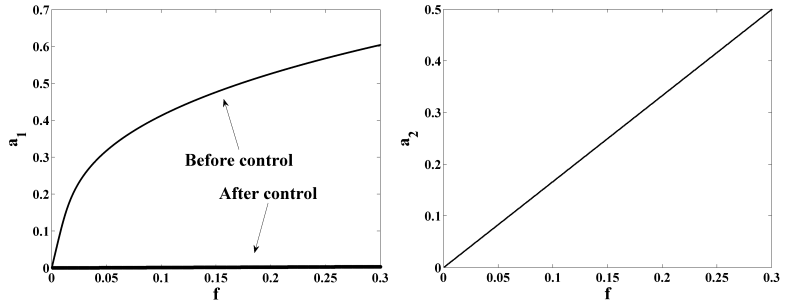

FIGURE 13. Force response curves of the main system and controller at different values of $\sigma_1 = \sigma_2 = 0$

derived to describe the nonlinear behavior of the amplitudes and phases of the main system and controller. A stability analysis was performed to determine the stable and unstable regions of operation for both the main system and the controller and then, the effects of varying different parameters on them were studied. The analysis showed that:

(1) After control, two peaks are located but they were separated by a bandwidth. This bandwidth can be controlled (widened or narrowed) by controlling the control signal gain c_1 and the feedback signal gain c_2.
(2) The peaks amplitudes of both the main system and the controller decreases by increasing the controller-damping coefficient μ_2, while the main system amplitude increases slightly at $\sigma_1 = 0$. This variation exhibited a case of saturation for the size of the bandwidth.
(3) For an optimum performance of operation of PPF controller, the natural frequency of the controller ω_2 should be tuned to the measured value of the excitation frequency Ω. Therefore, we can guarantee the validity of the relation $-0.1 \leq \sigma_2 = \sigma_1 \leq 0.1$, which made the amplitudes of both the main system and the controller at minimum levels.
(4) In case of mistuning, the variation of the detuning parameter σ_2 in the range $-0.1 \leq \sigma_2 \leq 0.1$ was good for the main system amplitude to be at small values less than 0.055.
(5) The relation between the main system amplitude and the excitation force became almost horizontal denoting a saturation case for the main system amplitude while the controller amplitude increased linearly with the excitation force.

In previous work regarding vibration control of the magnetically levitated body [1], Jo and Yabuno proposed a new type of a nonlinear passive vibration absorber that was connected to the main system. They designed it at a natural frequency in the neighborhood of twice that of the main system. They showed experimentally that the nonlinear vibration absorber has reduced the primary resonance amplitude by about 45%. This means that the controller effectiveness is about 2. A case of parametric resonance is studied in [2] for the same model, the steady state amplitude became close to zero by applying the same absorber in [1]. PPF controller was applied for vibrations of a nonlinear cantilever beam in [14]. El-Ganaini et al. showed that it is necessary to tune the controller natural frequency to the external

excitation one. They concluded that the controller effectiveness is about 625.
In the present work, a PPF controller was applied to reduce the vibrations of the magnetic levitation system shown in Fig. 1. If the natural frequency of the controller ω_2 was tuned to the measured value of the excitation frequency Ω, then the perfect tuning is done ($\sigma_1 = \sigma_2$) and the system amplitude was at its minimum level. It was also noticed from Fig. 12 that the best range of minimum system amplitudes for the perfect tuning is $-0.1 \leq \sigma_2 = \sigma_1 \leq 0.1$ where the controller effectiveness E_a is about 226. The analysis also revealed that the bandwidth could be controlled by the control signal gain c_1 and the feedback signal gain c_2. Increasing the linear damping of the controller μ_2 decreases the system peaks amplitudes but also increased the minimum main system amplitude slightly. Finally, the relation between the system amplitude and the excitation force became horizontal near zero value denoting a saturation case for the system amplitude.

Appendix

$$
\begin{aligned}
&r_{11} = -\mu_1, \quad r_{12} = \frac{k_1 f}{2}\cos\varphi_1, \quad r_{13} = \frac{c_1}{2}\sin\varphi_2, \quad r_{14} = \frac{c_1}{2}a_2\cos\varphi_2,\\
&r_{21} = -\frac{3\alpha}{4}a_1 - \frac{c_1}{2}\frac{a_2}{a_1^2}\cos\varphi_2 - \frac{k_1 f}{2a_1^2}\cos\varphi_1, \quad r_{22} = -\frac{k_1 f}{2a_1}\sin\varphi_1,\\
&r_{23} = \frac{c_1}{2a_1}\cos\varphi_2, \quad r_{24} = -\frac{c_1}{2}\frac{a_2}{a_1}\sin\varphi_2,\\
&r_{31} = -\frac{c_2}{2\omega_2}\sin\varphi_2, \quad r_{32} = 0, \quad r_{33} = -\mu_2, \quad r_{34} = -\frac{c_2}{2\omega_2}a_1\cos\varphi_2,\\
&r_{41} = -\frac{3\alpha}{4}a_1 - \frac{c_1}{2}\frac{a_2}{a_1^2}\cos\varphi_2 - \frac{k_1 f}{2a_1^2}\cos\varphi_1 - \frac{c_2}{2\omega_2 a_2}\cos\varphi_2, \quad r_{42} = -\frac{k_1 f}{2a_1}\sin\varphi_1,\\
&r_{43} = \frac{c_1}{2a_1}\cos\varphi_2 + \frac{c_2}{2\omega_2}\frac{a_1}{a_2^2}\cos\varphi_2, \quad r_{44} = -\frac{c_1}{2}\frac{a_2}{a_1}\sin\varphi_2 + \frac{c_2}{2\omega_2}\frac{a_1}{a_2}\sin\varphi_2\\
&\zeta_1 = -r_{11} - r_{22} - r_{33} - r_{44}\\
&\zeta_2 = r_{33}r_{44} - r_{21}r_{12} + r_{11}r_{44} - r_{42}r_{24} + r_{11}r_{33} - r_{31}r_{13} - r_{41}r_{14} - r_{32}r_{23} - r_{34}r_{43}\\
&\quad + r_{11}r_{22} + r_{22}r_{33} + r_{22}r_{44}\\
&\zeta_3 = r_{31}r_{12}r_{23} + r_{31}r_{13}r_{44} + r_{32}r_{23}r_{44} + r_{11}r_{32}r_{23} + r_{22}r_{34}r_{43} + r_{32}r_{43}r_{24} + r_{31}r_{43}r_{14}\\
&\quad + r_{21}r_{12}r_{44} + r_{21}r_{12}r_{33} + r_{11}r_{42}r_{24} - r_{11}r_{22}r_{44} - r_{11}r_{22}r_{33} + r_{21}r_{32}r_{13} + r_{31}r_{22}r_{13}\\
&\quad + r_{41}r_{12}r_{24} + r_{21}r_{42}r_{14} - r_{22}r_{33}r_{44} + r_{41}r_{14}r_{33} + r_{41}r_{13}r_{34} + r_{41}r_{22}r_{14} + r_{42}r_{23}r_{34}\\
&\quad + r_{42}r_{24}r_{33} - r_{11}r_{33}r_{44} + r_{11}r_{34}r_{43}\\
&\zeta_4 = r_{11}r_{22}r_{33}r_{44} - r_{11}r_{22}r_{34}r_{43} - r_{11}r_{32}r_{43}r_{24} - r_{11}r_{32}r_{23}r_{44} - r_{11}r_{42}r_{23}r_{34}\\
&\quad - r_{11}r_{42}r_{24}r_{33} - r_{21}r_{12}r_{33}r_{44} + r_{21}r_{12}r_{34}r_{43} - r_{21}r_{32}r_{43}r_{14} - r_{21}r_{32}r_{13}r_{44}\\
&\quad - r_{21}r_{42}r_{13}r_{34} - r_{21}r_{42}r_{14}r_{33} - r_{31}r_{12}r_{23}r_{44} - r_{31}r_{12}r_{43}r_{24} - r_{31}r_{22}r_{43}r_{14}\\
&\quad - r_{31}r_{22}r_{13}r_{44} + r_{31}r_{42}r_{13}r_{24} - r_{31}r_{42}r_{23}r_{14} - r_{41}r_{12}r_{23}r_{34} - r_{41}r_{12}r_{24}r_{33}\\
&\quad - r_{41}r_{22}r_{14}r_{33} - r_{41}r_{22}r_{13}r_{34} - r_{41}r_{32}r_{13}r_{24} + r_{41}r_{32}r_{23}r_{14}
\end{aligned}
$$

References

[1] Jo H., Yabuno H.: Amplitude reduction of primary resonance of nonlinear oscillator by a dynamic vibration absorber using nonlinear coupling. Nonlinear Dyn. **55**, 67-78 (2009)

[2] Jo H., Yabuno H.: Amplitude reduction of parametric resonance by dynamic vibration absorber based on quadratic nonlinear coupling. Journal of Sound and Vibration **329**, 2205-2217(2010)

[3] Yabuno H., Jo H.: Parametric resonance due to asymmetric nonlinearity of restoring force. Journal of System Design and Dynamics Vol.2 No.3 898-907 (2008)

[4] Warminski J., Bochenski M., Jarzyna W., Filipek P., Augustyniak M.: Active suppression of nonlinear composite beam vibrations by selected control algorithms. Commun Nonlinear Sci Numer Simulat **16**, 2237-2248 (2011)

[5] Shin C., Hong C., Jeong W. B.: Active vibration control of clamped beams using positive position feedback controllers with moment pair. Journal of Mechanical Science and Technology **26 (3)**, 731-740 (2012)

[6] Eissa M., Sayed M.: A comparison between active and passive vibration control of nonlinear simple pendulum, Part I: transversally tuned absorber and negative $G\dot{\varphi}^n$ feedback. Mathematical and Computational Applications, Vol. 11, No. 2, pp. 137-149 (2006)

[7] Eissa M., Sayed M.: A comparison between active and passive vibration control of non-linear simple pendulum, Part II: Longitudinal tuned absorber and negative $G\ddot{\varphi}$ and $G\varphi^n$ feedback. Mathematical and Computational Applications, Vol. 11, No. 2, pp. 151-162 (2006)

[8] Eissa M., Sayed M.: Vibration reduction of a three DOF non-linear spring pendulum. Communications in Nonlinear Science and Numerical Simulation **13**, 465-488 (2008)

[9] Eissa M., Bauomy H. S., Amer Y. A.: Active control of an aircraft tail subject to harmonic excitation. Acta Mech Sin **23**, 451-462 (2007)

[10] Amer Y.A., Bauomy H.S., Sayed M.: Vibration suppression in a twin-tail system to parametric and external excitation. Computers and Mathematics with Applications **58**, 1947_1964 (2009)

[11] Sayed M., Kamel M.: 1:2 and 1:3 internal resonance active absorber for non-linear vibrating system. Applied Mathematical Modelling **36**, 310-332 (2012)

[12] El-Ganaini W.A.A., El-Gohary H.A.: Vibration suppression via time-delay absorber described by non-linear differential equations. Adv. Theor. Appl. Mech., Vol. 4, , no. 2, 49 - 67 (2011)

[13] El-Gohary H.A., El-Ganaini W.A.A.: Vibration suppression of a dynamical system to multi-parametric excitations via time delay absorber. Applied Mathematical Modelling **36**, 35-45 (2012)

[14] El-Ganaini W. A., Saeed N. A., Eissa M.: Positive position feedback controller (PPF) for suppression of nonlinear sytem vibration. Nonlinear Dyn. **72**, 517-537 (2013)

[15] Eissa M., Saeed N. A.: Nonlinear vibration control of a horizontally supported Jeffcott-rotor system. Journal of Vibration and Control (2017), DOI: 10.1177/1077546317693928.

[16] Saeed N. A., kamel M.: Active magnetic bearing-based tuned controller to suppress lateral vibrations of a nonlinear Jeffcott-rotor system, Nonlinear Dynamics 90(1), 457-478 (2017)

[17] Nayfeh A. H., Mook D. T.: Nonlinear Oscillations. Wiley, New York (1995)

W. A. El-Ganaini

Department of Physics and Engineering Mathematics, Faculty of Electronic Engineering, Menoufia University, Menouf, 32952, Egypt.

E-mail address: wedad.ali.el.ganaini@gmail.com